J. Appl. Comput. Mech., 7(2) (2021) 935-943
DOI: 10.22055/JACM.2021.35920.2761

ISSN: 2383-4536
jacm.scu.ac.ir

Shahid Chamran University of Ahvaz

Journal of Applied and Computational Mechanics

Research Paper

Unsteady MHD Mixed Convection Flow of Water over a Sphere with Mass Transfer

A. Sahaya Jenifer[1], P. Saikrishnan[1], Roland W. Lewis[2]

[1] Department of Mathematics, National Institute of Technology, Tiruchirappalli, India, Emails: sahayajenifer496@gmail.com, psai@nitt.edu

[2] College of Engineering, Swansea University, Swansea, United Kingdom, Email: r.w.lewis@swansea.ac.uk

Received November 30 2020; Revised January 11 2021; Accepted for publication January 11 2021.
Corresponding author: P. Saikrishnan (psai@nitt.edu)

Abstract. This paper examines the unsteady magnetohydrodynamic (MHD) mixed convection flow over a sphere combined with variable fluid properties. An implicit finite difference scheme, together with the quasi-linearization, is used to find non-similar solutions for the governing equations. The vanishing skin friction is prevented or at least delayed by enhancing the mixed convection in both the cases of steady and unsteady fluid flow. Both skin friction and heat transfer coefficients are found to be increasing with an increase in time or MHD parameter.

Keywords: Unsteady flow, Mixed convection, MHD, Sphere, Variable properties, Non-similar solution

1. Introduction

The boundary layer flow problem holds rich implications in engineering, astrophysics, and the study of meteorological sciences. The physical model of flow over bluff bodies is applied in the design of cooling towers used in steel and oil industries, cooling of electronic chips, cooling circuit of nuclear reactors, heat exchangers, spinners in food processing industries. In particular, the spherical geometry is used in nuclear/radioactive waste disposal.

There is a substantial variation in fluid properties owing to the presence of a temperature gradient across a fluid medium. This temperature variation may be due to heat transfer when the fluid and the surface have dissimilarity in temperature or when there is a loss of heat present in the form of latent energy upon its liberation [1]. Together with these varying physical properties, the process of heat transfer for a variety of objects has already been thoughtfully analyzed by a significant number of researchers [2–8].

The mass transfer through a wall slot holds several tremendous practical implications in thermal protection, fuel injecting system of ramjets, drying theory, galvanizing the innermost section of the boundary layer in adverse pressure gradients and reducing skin friction on high-speed aircraft [9–11]. Uniform suction(injection) creates discontinuities at the ends of slot. An ultimate solution to overcome this is by implementing a non-uniform suction(injection), as given in [12]. In the past two decades, numerous investigations, including the impact of non-uniform mass transfer, have been carried out in [3–7, 10, 13].

The boundary-layer flows are found to be both unsteady and non-similar in nature. The unsteadiness and non-similarity that occur may be due to the body's curvature or the velocity profiles at the boundary or due to the surface mass transfer, or perhaps an amalgamation of all the factors mentioned above. A vast majority of the researchers confined their works to unsteady self-similar flows or steady non-similar flows due to mathematical complexities. A brief review of methods to find non-similar solutions for steady flows and the references of apposite works done up till 1967 has been stated in [14]. Since then, several researchers undertook investigations over steady incompressible laminar non-similar flows.

On the other hand, the unsteady flow has been a topic of discussion for many researchers [15–17]. An improved finite volume scheme has been proposed in [18] for unsteady viscous incompressible flows. In [19], authors have investigated the non-similar solution of unsteady two-dimensional and axisymmetric water boundary layers with variable viscosity and Prandtl number. Taking non-uniform mass transfer into account, [5] worked on a non-similar solution for unsteady fluid flow over a sphere.

In [13, 20–26], the authors have analyzed the effect of mixed convection on steady or unsteady fluid flow over various bodies. On the other hand, MHD's effect on steady or unsteady fluid flow has been observed in [27–30]. The above studies were focused on analyzing the flow problem with either mixed convection or magnetic field. The cumulative impact of MHD and mixed convection on a steady flow of fluid is observed in [4, 10, 31, 32] over a flat vertical plate, vertical wedge, sphere and vertical elastic sheet, respectively. Recently, taking unsteadiness into consideration, an investigation of MHD mixed convective flow is done across an exponentially stretching surface, a vertical wedge, a moving vertical plate, and a sliced magnetic sphere respectively, in [33-36]. Emerging trends on unsteady mixed convective/free convective flow of some nanofluids past various bluff bodies under the influence of magnetic field has been observed in [37-39].

The present study focuses on obtaining non-similar solutions of unsteady MHD mixed convection fluid flow problems with variable physical properties and non-uniform mass transfer. The fluid considered here is water due to its extreme practical applications in engineering.

Published online: January 12 2021

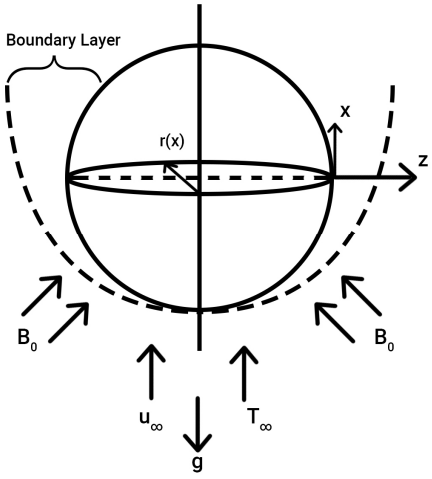

Fig. 1. Boundary layer flow model

2. Mathematical Formulation

The flow model of unsteady laminar non-similar boundary layer over a sphere of radius R is presented in Fig. 1. The curvilinear coordinates are x and z, respectively, along and perpendicular to the sphere's surface with u and w being the corresponding velocity components. A constant magnetic field B_0 is supposed to be acting in z –direction. Any other induced magnetic field is neglected in this study. It is assumed that mixed convective flow is in the upward direction, and the gravity g in the downward direction. The sphere's surface is considered electrically non-conducting and maintained at a constant temperature of T_w. The free stream flows with velocity u_∞ at a constant temperature T_∞ with $T_w > T_\infty$. The mass transfer is performed in the axial direction with the injecting fluid having same physical properties as water. The rate of suction/injection is taken to be low so that it will not affect the inviscid flow.

The variation of temperature between the free stream and the surface of the sphere is assumed to be less than 40. Within this temperature limit considered, the properties of water such as density (μ) and specific heat (c_p) vary up to a maximum of 1% and this minute variation allows the use of ρ and c_p as constants. On the other hand, properties such as viscosity and thermal conductivity vary significantly with temperature, and so does the Prandtl number. Both μ and Pr have an inverse linear relationship with temperature [19],

$$\mu = \frac{1}{b_1 + b_2 T} \text{ and } \Pr = \frac{1}{c_1 + c_2 T} \tag{1}$$

where

$$b_1 = 53.41,\ b_2 = 2.43,\ c_1 = 0.068,\ c_2 = 0.004 \tag{2}$$

Under these assumptions, the boundary layer flow is governed by the following equations[4,5,34]:

Continuity equation:

$$(ru)_x + (rw)_z = 0 \tag{3}$$

Momentum equation:

$$u_t + uu_x + wu_z = (u_e)_t + u_e(u_e)_x + \frac{1}{\rho}(\mu u_z)_z + g\beta(T - T_\infty)\sin\frac{x}{R} - \frac{\sigma B_0^2}{\rho}(u - u_e) \tag{4}$$

Energy equation:

$$T_t + uT_x + wT_z = \frac{1}{\rho}\left(\frac{\mu}{\Pr}T_z\right)_z + \frac{\mu}{\rho c_p}(u_z)^2 + \frac{\sigma B_0^2}{\rho c_p}(u^2 - u_e u) \tag{5}$$

Initial conditions:

$$u(x,z,0) = u_i(x,z), \quad w(x,z,0) = w_i(x,z), \quad T(x,z,0) = T_i(x,z) \tag{6}$$

Boundary conditions:

$$\begin{aligned} u(x,0,t) &= 0, & w(x,0,t) &= w_w(x,t), & T(x,0,t) &= T_w \\ u(x,\infty,t) &= u_e(x,t), & & & T(x,\infty,t) &= T_\infty \end{aligned} \tag{7}$$

To convert the Eqs. (3)-(5) into a non-dimensional form, the following transformations are used.

$$\xi = \int_0^x \frac{U}{u_\infty}\left(\frac{x}{R}\right)^2 d\left(\frac{x}{R}\right), \qquad t^* = \frac{3}{2}\mathrm{Re}\left(\frac{\mu_e}{\rho R^2}\right)t$$
$$\eta = \frac{U}{u_\infty}\left(\frac{\mathrm{Re}}{2\xi}\right)^{1/2}\left(\frac{r}{R}\right)\left(\frac{z}{R}\right), \qquad \mathrm{Re} = \frac{u_\infty R}{\nu}$$
$$\psi(x,z,t) = u_\infty R\left(\frac{2\xi}{\mathrm{Re}}\right)^{1/2}\varphi(t^*)f(\xi,\eta,t^*), \qquad \varphi(t^*) = 1+\varepsilon t^{*^2} \tag{8}$$
$$u = \frac{R}{r}\psi_z, \qquad w = -\frac{R}{r}\psi_x, \qquad G = \frac{T-T_\infty}{T_w-T_\infty}, \varepsilon = 0.25$$

The above transformations satisfy eq. (3) identically and convert the Eqs. (4) and (5) to non-dimensional form as follows:

$$(NF_\eta)_\eta + \varphi\left[fF_\eta + \beta(1-F^2)\right] - P\left[F_{t^*} - \varphi^{-1}\varphi_{t^*}(1-F)\right] + \varphi^{-1}\lambda S_1(\xi)G + MP(1-F) = 2\xi\varphi(FF_\xi - f_\xi F_\eta) \tag{9}$$

$$\left(\frac{1}{\mathrm{Pr}}NG_\eta\right)_\eta + \varphi f G_\eta - PG_{t^*} + N\left(\frac{u_e}{u_\infty}\right)^2 \mathrm{Ec}F_\eta^2 + \left(\frac{u_e}{u_\infty}\right)^2 P\,\mathrm{Ec}MF(F-1) = 2\xi\varphi(FG_\xi - f_\xi G_\eta) \tag{10}$$

with

$$F(\xi,0,t^*) = 0, \qquad G(\xi,0,t^*) = 1, \qquad F(\xi,\infty,t^*) = 1, \qquad G(\xi,\infty,t^*) = 0 \tag{11}$$

where

$$N = \frac{\mu}{\mu_\infty} = \frac{b_1+b_2T_\infty}{b_1+b_2T} = \frac{1}{1+a_1G}, \qquad \mathrm{Pr} = \frac{1}{c_1+c_2T} = \frac{1}{a_2+a_3G},$$
$$a_1 = \frac{b_2\Delta T_w}{b_1+b_2T_\infty}, \qquad a_2 = c_1+c_2T_\infty, \qquad a_3 = c_2\Delta T_w,$$
$$\Delta T_w = T_w - T_\infty, \qquad \frac{u}{u_e} = f_\eta = F, \qquad u_e = U\varphi(t^*),$$
$$\mathrm{Ec} = \frac{u_\infty^2}{c_p\Delta T_w}, \qquad f = \int_0^\eta F\,d\eta + f_w, \qquad \beta(\xi) = \frac{2\xi}{U}\frac{dU}{d\xi},$$
$$P = 3\xi\left(\frac{R}{r}\right)^2\left(\frac{u_\infty}{U}\right)^2, \qquad \alpha_1 = \frac{2\xi}{r}\frac{dr}{d\xi}, \qquad M = \frac{2}{3}\frac{\sigma B_0^2 R}{\rho\mu_\infty}, \tag{12}$$
$$S_1(\xi) = 2\xi\left(\frac{u_\infty}{U}\right)^3\left(\frac{R}{r}\right), \qquad \lambda = \frac{Gr}{\mathrm{Re}^2}, \qquad Gr = \frac{g\beta R^3\Delta T_w}{\nu_\infty^2},$$
$$\nu_\infty = \frac{\mu_\infty}{\rho}, \qquad w = -\frac{r}{R}(2\xi\,\mathrm{Re})^{-1/2}U\varphi\left[f + 2\xi f_\xi + (\beta+\alpha_1-1)\eta F\right],$$
$$f_w = -\xi^{-1/2}\left(\frac{\mathrm{Re}}{2}\right)^{1/2}\varphi^{-1}\int_0^x \frac{w_w(x,t^*)}{u_\infty}\left(\frac{r}{R}\right)d\left(\frac{x}{R}\right)$$

The velocity distribution at the boundary layer's edge is written as,

$$\frac{u_e}{u_\infty} = \frac{3}{2}\sin\bar{x}\,\varphi(t^*), \quad \frac{U}{u_\infty} = \frac{3}{2}\sin\bar{x},$$
$$\bar{x} = \frac{x}{R}, \quad \frac{r}{R} = \sin\bar{x} \tag{13}$$

Hence ξ, $\beta(\xi)$, $P(\xi)$, $\alpha_1(\xi)$ and $S_1(\xi)$ can be written as expressions in $\bar{x}$ as follows.

$$\xi = \frac{B_1^2B_3}{2}, \qquad \beta = \frac{2}{3}\cos\bar{x}\,B_3B_2^{-2}, \quad P = \frac{2}{3}B_2^{-2}B_3,$$
$$\alpha_1 = \beta, \quad S_1 = \frac{8}{27}B_2^{-2}B_3 \tag{14}$$

where

$$B_1 = 1-\cos\bar{x}, \qquad B_2 = 1+\cos\bar{x}, \qquad B_3 = 2+\cos\bar{x} \tag{15}$$

The value of f_w is given by

$$f_w = \begin{cases} 0, & \bar{x} \le \bar{x_0} \\ A\varphi^{-1}(B_1)^{-1}(B_3)^{-1/2}C(\bar{x},\bar{x_0}), & \bar{x} \in \left[\bar{x_0},\bar{x_0^*}\right] \\ A\varphi^{-1}(B_1)^{-1}(B_3)^{-1/2}C(\bar{x_0^*},\bar{x_0}), & \text{otherwise} \end{cases} \tag{16}$$

where the function

$$C(\bar{x},\overline{x_0}) = \frac{\sin\left[(\omega^*-1)\bar{x}-\omega^*\overline{x_0}\right]+\sin\overline{x_0}}{(\omega^*-1)} - \frac{\sin\left[(\omega^*+1)\bar{x}-\omega^*\overline{x_0}\right]-\sin\overline{x_0}}{(\omega^*+1)} \tag{17}$$

Here, w_w is taken as

$$w_w = \begin{cases} -u_\infty\left(\frac{\mathrm{Re}}{2}\right)^{-1/2} A\,2^{1/2}\sin\left[\omega^*(\bar{x}-\overline{x_0})\right], & \bar{x}\in\left[\overline{x_0},\overline{x_0^*}\right] \\ 0, & \text{otherwise} \end{cases} \tag{18}$$

It is convenient to write the equations in $\bar{x}$ instead of ξ. The relation between ξ and $\bar{x}$ is found to be

$$\xi\frac{\partial}{\partial\xi} = B(\bar{x})\frac{\partial}{\partial\bar{x}} \tag{19}$$

where,

$$B(\bar{x}) = \frac{1}{3}\tan\frac{\bar{x}}{2}B_3B_2^{-1} \tag{20}$$

Substituting Eqs. (19) and (20) in the Eqs. (9) and (10), we obtain the dimensionless equations,

$$(NF_\eta)_\eta + \varphi\left[fF_\eta + \beta(1-F^2)\right] - P\left[F_{t^*} - \varphi^{-1}\varphi_{t^*}(1-F)\right] + \varphi^{-1}\lambda S_1(\bar{x})G + MP(1-F) = 2B(\bar{x})\varphi(FF_{\bar{x}} - f_{\bar{x}}F_\eta) \tag{21}$$

$$\left(\frac{1}{\mathrm{Pr}}NG_\eta\right)_\eta + \varphi fG_\eta - PG_{t^*} + N\left(\frac{u_e}{u_\infty}\right)^2 EcF_\eta^2 + \left(\frac{u_e}{u_\infty}\right)^2 PEcMF(F-1) = 2B(\bar{x})\varphi(FG_{\bar{x}} - f_{\bar{x}}G_\eta) \tag{22}$$

The boundary conditions become

$$F(\bar{x},0,t^*) = 0, \qquad G(\bar{x},0,t^*) = 1, \qquad F(\bar{x},\infty,t^*) = 1, \qquad G(\bar{x},\infty,t^*) = 0 \tag{23}$$

The skin friction coefficient and the heat transfer coefficient at the wall can be expressed as

$$\begin{aligned} C_f(\mathrm{Re})^{1/2} &= \frac{9}{2}\sin\bar{x}B_2B_3^{-1/2}\varphi(t^*)N_w(F_\eta)_w \\ Nu(\mathrm{Re})^{-1/2} &= -\frac{3}{2}B_2B_3^{-1/2}(G_\eta)_w \end{aligned} \tag{24}$$

where,

$$C_f = \frac{2\left[\mu\left(\frac{\partial u}{\partial z}\right)\right]_w}{\rho u_\infty^2}, \qquad Nu = \frac{R\left(\frac{\partial T}{\partial z}\right)_w}{(T_\infty - T_w)}, \qquad N_w = \frac{1}{1+a_1G_w} \tag{25}$$

3. Numerical Method

The quasi-linearization method is utilized to linearize the non-linear PDEs (21) and (22). The resulting sequence of linear differential equations are:

$$\begin{aligned} &K_1^nF_{\eta\eta}^{n+1} + K_2^nF_\eta^{n+1} + K_3^nF^{n+1} + K_4^nF_\xi^{n+1} + K_5^nF_{t^*}^{n+1} + K_6^nG_\eta^{n+1} + K_7^nG^{n+1} = K_8^n \\ &L_1^nG_{\eta\eta}^{n+1} + L_2^nG_\eta^{n+1} + L_3^nG^{n+1} + L_4^nG_\xi^{n+1} + L_5^nG_{t^*}^{n+1} + L_6^nF_\eta^{n+1} + L_7^nF^{n+1} = L_8^n \end{aligned} \tag{26}$$

with the coefficients,

$K_1 = N$
$K_2 = -a_1G_\eta N^2 + \varphi f + 2\xi\varphi f_\xi$
$K_3 = -2\varphi\beta F - P\varphi^{-1}\varphi_{t^*} - MP - 2\xi\varphi F_\xi$
$K_4 = -2\xi\varphi F$
$K_5 = -a_1F_\eta N^2$
$K_6 = \varphi^{-1}\lambda S_1 + 2a_1^2N^3F_\eta G_\eta - a_1F_{\eta\eta}N^2$
$K_7 = -P$
$K_8 = -\varphi\beta(1+F^2) - P\varphi^{-1}\varphi_{t^*} - MP + 2a_1^2N^3F_\eta G_\eta G - a_1F_{\eta\eta}N^2G - a_1F_\eta G_\eta N^2 - 2\xi\varphi FF_\xi$

$$L_1 = \frac{N}{\Pr}$$

$$L_2 = \varphi f + 2\xi\varphi f_\xi + 2\left(a_3 N - \frac{a_1 N^2}{\Pr}\right)G_\eta$$

$$L_3 = -a_1 N^2\left(\frac{u_e}{u_\infty}\right)^2 Ec F_\eta^2 - 2\left(a_1 a_3 N^2 - \frac{{a_1}^2 N^3}{\Pr}\right){G_\eta}^2 - \frac{a_1 N^2}{\Pr}G_{\eta\eta} + a_3 N G_{\eta\eta}$$

$$L_4 = -2\xi\varphi F$$

$$L_5 = 2N\left(\frac{u_e}{u_\infty}\right)^2 Ec F_\eta$$

$$L_6 = \left(\frac{u_e}{u_\infty}\right)^2 PEcM(2F-1) - 2\xi\varphi G_\xi$$

$$L_7 = -P$$

$$L_8 = -a_1 N^2\left(\frac{u_e}{u_\infty}\right)^2 Ec F_\eta^2 G + N\left(\frac{u_e}{u_\infty}\right)^2 Ec F_\eta^2 - 2\left(a_1 a_3 N^2 - \frac{{a_1}^2 N^3}{\Pr}\right){G_\eta}^2 G + \left(-\frac{a_1 N^2}{\Pr} + a_3 N\right)G_{\eta\eta} G + \left(-\frac{a_1 N^2}{\Pr} + a_3 N\right)G_\eta^2 + \left(\frac{u_e}{u_\infty}\right)^2 PEcMF^2 - 2\xi\varphi F G_\xi$$

The coefficients at the index of iteration n is assumed to be known and the results are to be calculated at $n+1$. Implicit finite difference method is employed to eq. (1.26) and is written as a block tri-diagonal system as given in [40]. Finally, Varga's algorithm [41] is implemented to solve the system with step sizes $\Delta\eta = 10^{-2}, \Delta\bar{x} = 5\times10^{-4}$ and $\Delta t^* = 10^{-2}$ in their respective directions. Here, η_∞ is taken as 6. The convergence of solution is achieved if the following condition is satisfied.

$$b_1 = 53.41,\ b_2 = 2.43,\ c_1 = 0.068,\ c_2 = 0.004 \tag{27}$$

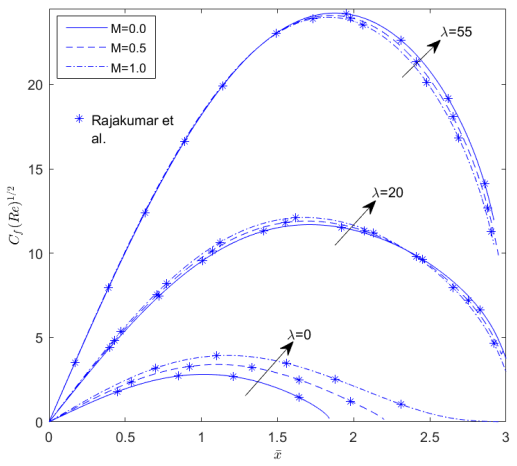

Fig. 2. Comparison of the skin friction coefficient for a steady flow with various values of M and λ with those of [4] where $A = 0,\ Ec = 0$

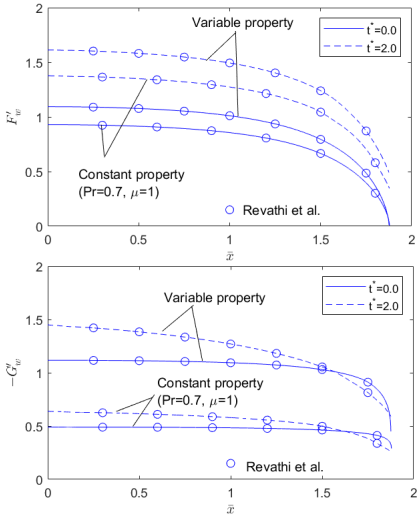

Fig. 3. Comparison of the skin friction and the heat transfer parameters for constant and fluid properties with those of [5] where $A = 0, Ec = 0, \lambda = 0, M = 0$

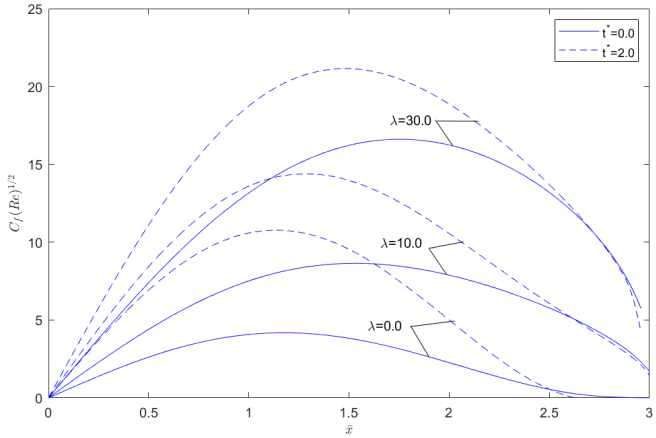

Fig. 4. Effect of the mixed convection parameter λ on the skin friction coefficient for $A = 0, M = 1, Ec = 0$

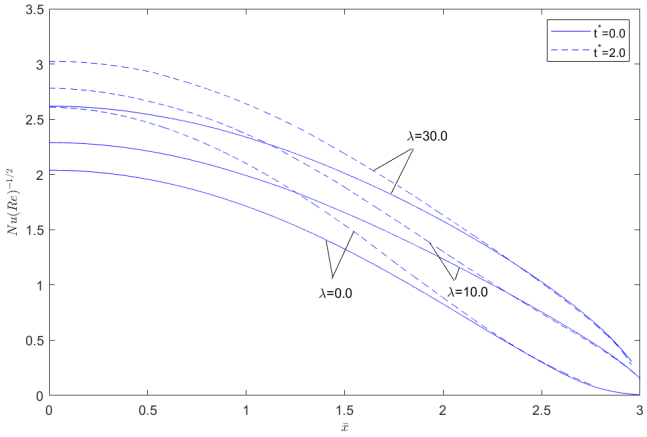

Fig. 5. Effect of the mixed convection parameter λ on the heat transfer coefficient for $A = 0, M = 1, Ec = 0$

4. Results and Discussions

To assure the precision of our study, in both steady as well as unsteady cases, the obtained solutions are compared with those available in the literature. In the case of steady flow, Fig. 2 depicts various MHD and mixed convection parameters' impact on the skin friction coefficient and the results are compared with [4]. Also, in Fig. 3, the skin friction and heat transfer parameters $\left[F'_w, G'_w\right]$ at different times for constant and variable properties with $\lambda = 0, M = 0$ have been shown and are compared with [5]. It is observed that the solutions agree with all the studies mentioned above.

Figures 4 and 5 show the variation of the skin friction coefficient $\left[C_f(\mathrm{Re})^{1/2}\right]$ and the heat transfer coefficient $\left[Nu(\mathrm{Re})^{-1/2}\right]$ due to the mixed convection parameter λ over time with the accompanying magnetic field $(M = 1)$ for $\Delta T_w = 10.0^\circ C, T_\infty = 18.7^\circ C, A = 0, Ec = 0$. It is noted that $C_f(\mathrm{Re})^{1/2}$ and $Nu(\mathrm{Re})^{-1/2}$ increase as λ or t^* increases. The mixed convection parameter λ has prominent effects on $C_f(\mathrm{Re})^{1/2}$ than on $Nu(\mathrm{Re})^{-1/2}$; this is because $\lambda > 0$ gives rise to a favorable pressure gradient and $C_f(\mathrm{Re})^{1/2}$ depends strongly on the pressure gradient. It can be further noted that enhancing λ prevents the skin friction coefficient from vanishing at both times $t^* = 0.0$ and $t^* = 2.0$.

At $\bar{x} = 1.5$, as λ changes from 0 to 30, the skin friction coefficient depicts an upsurge of about 323.83% at $t^* = 0.0$ and about 121.52% at $t^* = 2.0$ and an increase in the heat transfer coefficient of about 51.7% at $t^* = 0.0$ and about 41.83% at $t^* = 2.0$ is observed.

Figures 6 and 7 show that $C_f(\mathrm{Re})^{1/2}$ and $Nu(\mathrm{Re})^{-1/2}$ increase with an increase in t^* and with the enhancing of MHD parameter M for a fixed $\lambda = 20$. The MHD parameter's impact is not prominent on $Nu(\mathrm{Re})^{-1/2}$ in the steady case. However, the significance is notable with an increase of t^* . Due to the strong presence of the mixed convection parameter, skin friction is prevented from vanishing, irrespective of the value of M .

At $\bar{x} = 1.5$, as M changes from 0 to 1, $C_f(\mathrm{Re})^{1/2}$ registers an increase of 4.47% and 9.52%; $Nu(\mathrm{Re})^{-1/2}$ registers an increase of 0.86% and 2.33%, respectively at $t^* = 0.0$ and 2.0.

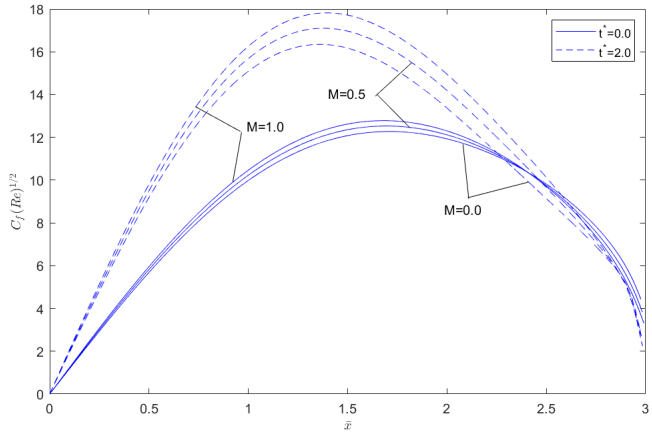

Fig. 6. Effect of the MHD parameter M on the skin friction coefficient for $A = 0, \lambda = 20, Ec = 0$

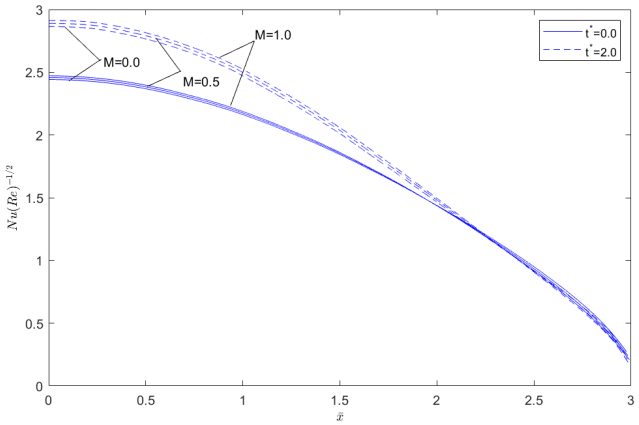

Fig. 7. Effect of the MHD parameter M on the heat transfer coefficient for $A = 0, \lambda = 20, Ec = 0$

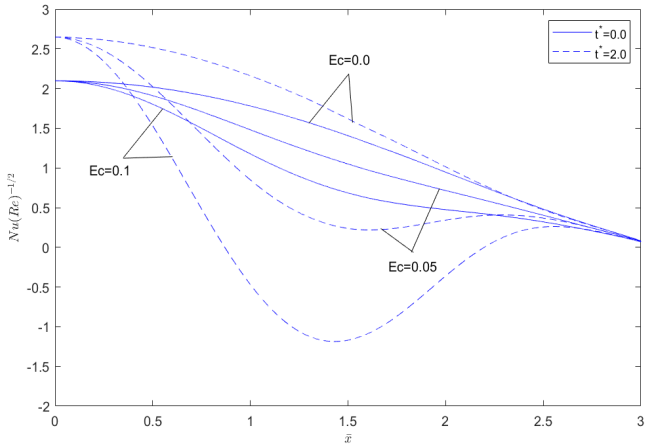

Fig. 8. Effect of the viscous dissipation parameter Ec on the heat transfer coefficient for $A = 0, \lambda = 2, Ec = 0$

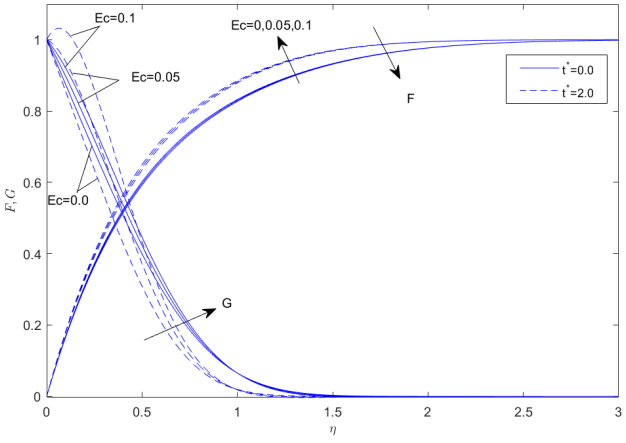

Fig. 9. Effect of the viscous dissipation parameter Ec on the velocity profile and the temperature profile for $A = 0, \lambda = 2, Ec = 0$

In Fig. 8, the viscous dissipation parameter Ec 's impact on $Nu(\mathrm{Re})^{-1/2}$ for $A=0, M=1, \lambda=2$ can be seen. It is observed that, in the presence of MHD and mixed convection parameters, Ec has prominent effects on the heat transfer coefficient, whereas it barely affects the skin friction coefficient in both steady and unsteady cases and hence the corresponding figure is not presented here. The reason for this is the energy equation depends explicitly on Ec while the momentum equation does not. $Nu(\mathrm{Re})^{-1/2}$ decreases with the increase of t^* and $Ec>0$.

Even for a small change of Ec from 0 to 0.1, at $\bar{x}=1.5$, $Nu(\mathrm{Re})^{-1/2}$ decreases by about 51.28% at $t^*=0.0$ and about 172.22% at $t^*=2.0$.

From Fig. 9, at $\bar{x}=1.5$, Ec shows prominent effects on the temperature profile than on the velocity profile. For $Ec>0$ and $t^*=2$, owing to viscous dissipation, the temperature of the fluid near the wall rises higher than T_w, although originally, the wall was at a higher temperature. This results in the temperature profile surpassing 1 near the wall, after which it declines to zero. Nevertheless, such circumstance doesn't occur when $Ec=0$ or $t^*=0$.

The influence of non-uniform slot suction(injection) on $C_f(\mathrm{Re})^{1/2}$ and $Nu(\mathrm{Re})^{-1/2}$ at various streamwise locations $\bar{x}$ for $M=1, \lambda=5$ and for times $t^*=0.0$ and 2.0 have been shown in Figs. 10-13. For $t^*\geq 0$ and $A>0$ (suction) as the slot starts, $C_f(\mathrm{Re})^{1/2}$ and $Nu(\mathrm{Re})^{-1/2}$ increase remarkably and hit maximum value before reaching its trailing edge. After that, $C_f(\mathrm{Re})^{1/2}$ and $Nu(\mathrm{Re})^{-1/2}$ decrease and manage to stay finite for both steady and unsteady cases. While, on the contrary, injection $(A<0)$ has the opposite effect. However, irrespective of A, skin friction as well as heat transfer coefficients increase as time increases.

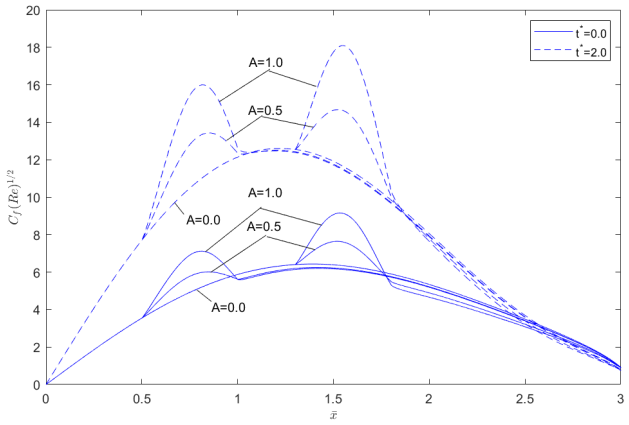

Fig. 10. Effects of suction and slot location $(\bar{x}=0.5,1.3)$ on the skin friction coefficient for $Ec=0, \lambda=5, M=1$

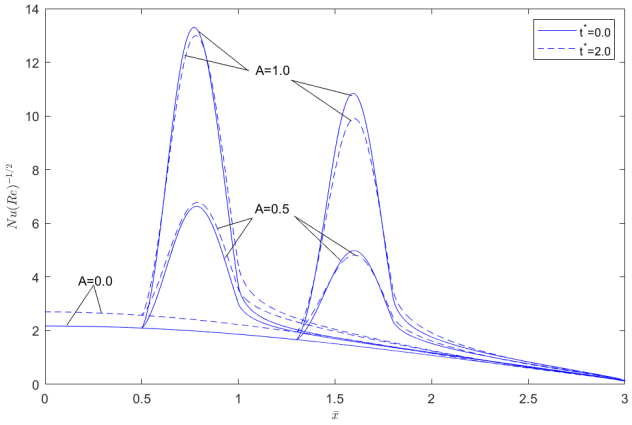

Fig. 11. Effects of suction and slot location $(\bar{x}=0.5,1.3)$ on the heat transfer coefficient for $Ec=0, \lambda=5, M=1$

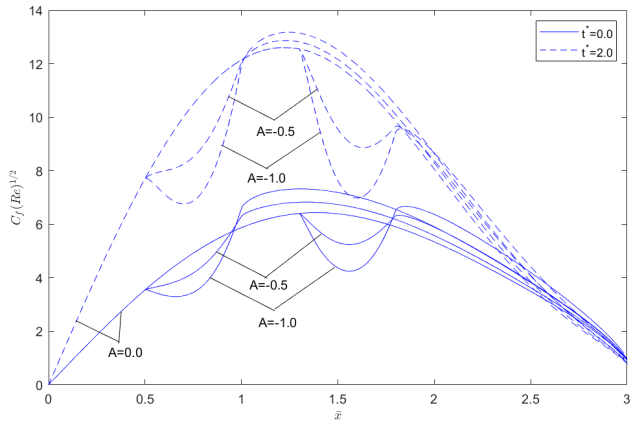

Fig. 12. Effects of injection and slot location $(\bar{x}=0.5,1.3)$ on the skin friction coefficient for $Ec=0, \lambda=5, M=1$

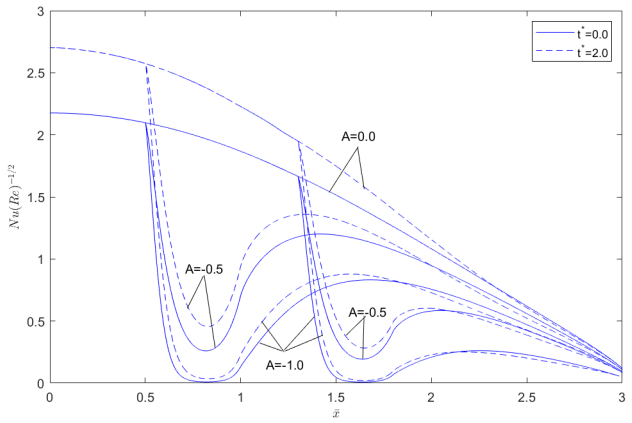

Fig. 13. Effects of injection and slot location $(\bar{x}=0.5,1.3)$ on the heat transfer coefficient $Ec=0, \lambda=5, M=1$

5. Conclusions

Non-similar solutions of an unsteady MHD mixed convection flow of water over a sphere are obtained numerically and the observations are as follows:

- The mixed convection parameter has more prominent impact on the skin friction coefficient than the heat transfer coefficient and the significance becomes less as the time increases.
- Enhancing the mixed convection parameter prevents zero skin friction in both steady and unsteady cases.
- The MHD parameter affects the skin friction and heat transfer coefficients noticeably in the unsteady case than it does in the steady case.
- The viscous dissipation parameter has prominent effects on the temperature profile than the velocity profile. An overshoot in the temperature profile has been observed in the unsteady case.
- Ec diminishes the heat transfer coefficient over time, whereas the effect is insignificant on the skin friction coefficient.
- The effect of unsteadiness, subject to slot suction, is more significant on the skin friction coefficient as compared to the heat transfer coefficient whereas, subject to slot injection, the effect is significant on both.

Author Contributions

P. Saikrishnan initiated the project, designed the model and computational framework; A. Sahaya Jenifer performed the calculations, wrote the manuscript; Roland W. Lewis examined the theory validation. The manuscript was written through the contribution of all authors. All authors discussed the results, reviewed, and approved the final version of the manuscript.

Conflict of Interest

The authors declared no potential conflicts of interest with respect to the research, authorship, and publication of this article.

Funding

The authors received no financial support for the research, authorship, and publication of this article.

Nomenclature

A	Dimensionless mass transfer parameter	N	Viscosity ratio
B_0	Magnetic field strength	Nu	Nusselt number
c_p	Specific heat at constant pressure	Pr	Prandtl number
C_f	Skin friction coefficient in the $x-$ direction	$r(x)$	Radius of the section normal to the axis of the sphere
Ec	Eckert number	R	Radius of the sphere
f	Dimensionless stream function	Re	Reynolds number
f_w	Surface mass transfer distribution	t	Dimensional time
F	Dimensionless velocity in the $x-$ direction	t^*	Dimensionless time
G	Dimensionless temperature	T	Temperature
g	Gravity	u,w	Dimensional velocity in $x,z-$ directions, respectively
Gr	Grashof number	U	Steady state velocity at the boundary layer's edge
k	Thermal conductivity	x,z	Dimensional meridional and normal distances
M	MHD parameter	$\bar{x}$	Dimensionless meridional distance
		$\overline{x_0},\overline{x_0^*}$	Ends of slot

Greek Symbols

$\beta(\xi)$	Pressure gradient	μ	Dynamic viscosity
β	Volumetric coefficient of thermal expansion	ρ	Density
$\Delta\eta,\Delta\bar{x},\Delta t^*$	Step sizes in $\eta,\bar{x},t^*$ directions, respectively	σ	Electrical conduction
η,ξ	Transformed coordinates	ψ	Dimensional stream function
ε	Constant used in the continuous function of time	ω^*	Slot length parameter
λ	Mixed convection parameter	φ	Continuous function of time

Subscripts

e	Conditions at edge of the boundary layer	∞	Conditions in the free stream
w	Conditions at the surface of the sphere	$x,z,\bar{x},\xi$	Partial derivatives with respect to these variables

References

[1] Schlichting, H., Gersten, K., *Boundary-Layer Theory,* Springer-Verlag Berlin Heidelberg, 2017.
[2] Molla, M.D., Saha, S., Hossain, A., The Effect of Temperature Dependent Viscosity on MHD Natural Convection Flow from an Isothermal Sphere, *Journal of Applied Fluid Mechanics*, 5(2), 2012, 25–31.
[3] Poornima, C., Ashwini, G., Eswara, A., Non-Uniform Slot Suction (Injection) into MHD Axisymmetric Boundary Layer Flow with Variable Viscosity, *International Journal of Mathematics*, 1(1), 2011, 78–85.
[4] Rajakumar, J., Saikrishnan, P., Chamkha, A., Non-Uniform Mass Transfer in MHD Mixed Convection Flow of Water over a Sphere with Variable Viscosity and Prandtl Number, *International Journal of Numerical Methods for Heat & Fluid Flow*, 26(7), 2016, 2235–2251.
[5] Revathi, G., Saikrishnan, P., Chamkha, A., Non-similar Solution for Unsteady Water Boundary Layer Flows over a Sphere with Non-uniform Mass Transfer, *International Journal of Numerical Methods for Heat & Fluid Flow*, 23(6), 2013, 1104–1116.
[6] Saikrishnan, P., Roy, S., Non-Uniform Slot Injection (Suction) into Water Boundary Layers over (i) a Cylinder and (ii) a Sphere, *International Journal of Engineering Science*, 41(12), 2003, 1351–1365.
[7] Saikrishnan, P., Roy, S., Steady Nonsimilar Axisymmetric Water Boundary Layers with Variable Viscosity and Prandtl Number, *Acta Mechanica*, 157(1), 2002, 187–199.
[8] Singh, A.K., Singh, A.K., Roy, S., Analysis of Mixed Convection in Water Boundary Layer Flows over a Moving Vertical Plate with Variable Viscosity and Prandtl Number, *International Journal of Numerical Methods for Heat & Fluid Flow*, 29(2), 2019, 602–616.
[9] Comini, G., Lewis, R.W., A Numerical Solution of Two-Dimensional Problems Involving Heat and Mass Transfer, *International Journal of Heat and Mass Transfer*, 19(12), 1976, 1387–1392.
[10] Ganapathirao, M., Chamkha, A., Nadiminti, S., Effects of Non-Uniform Slot Suction/Injection and Chemical Reaction on Mixed Convective MHD Flow along a Vertical Wedge Embedded in a Porous Medium, *Frontiers in Heat and Mass Transfer*, 13(1), 2019, 15.
[11] Nithiarasu, P., Lewis, R.W., Seetharamu, K.N., *Fundamentals of the Finite Element Method for Heat and Mass Transfer,* John Wiley & Sons, 2016.
[12] Minkowycz, W., Sparrow, E., Schneider, E., Pletcher, R., *Handbook of Numerical Heat Transfer,* John Wiley & Sons, 2006.
[13] Ganapathirao, M., Ravindran, R., Pop, I., Non-Uniform Slot Suction (Injection) on an Unsteady Mixed Convection Flow over a Wedge with Chemical Reaction and Heat Generation or Absorption, *International Journal of Heat and Mass Transfer*, 67(1), 2013, 1054–1061.
[14] Dewey, C.F., Gross, J.F., Exact Similar Solutions of the Laminar Boundary-Layer Equations, *Advances in Heat Transfer*, 4(1), 1967, 317–446.
[15] Hancock, G.J., Unsteady Boundary Layers, *IMA Journal of Applied Mathematics*, 32(1), 1984, 175–185.
[16] Ingham, D.B., Unsteady Separation, *Journal of Computational Physics*, 53(1), 1984, 90–99.

[17] Riley, N., Unsteady Laminar Boundary Layers, *SIAM Review*, 17(2), 1975, 274–297.
[18] Malan, A., Lewis, R.W., Nithiarasu, P., An Improved Unsteady, Unstructured, Artificial Compressibility, Finite Volume Scheme for Viscous Incompressible Flows: Part I. Theory and Implementation, *International Journal for Numerical Methods in Engineering,* 54(5), 2002, 695–714.
[19] Eswara, A.T., Nath, G., Unsteady Nonsimilar Two-Dimensional and Axisymmetric Water Boundary Layers with Variable Viscosity and Prandtl Number, *International Journal of Engineering Science*, 32(2), 1994, 267–279.
[20] Chen, T.S., Mucoglu, A., Analysis of Mixed Forced and Free Convection about a Sphere, *International Journal of Heat and Mass Transfer*, 20(8), 1977, 867–875.
[21] Devi, C.D.S., Nath, G., Unsteady Mixed Convection over Two-Dimensional and Axisymmetric Bodies, *Wärme- Und Stoffübertragung*, 22(1), 1988, 83–90.
[22] Ganapathirao, M., Revathi, G., Ravindran, R., Unsteady Mixed Convection Boundary Layer Flow over a Vertical Cone with Non-Uniform Slot Suction (Injection), *Meccanica*, 49(3), 2014, 673–686.
[23] Kumari, M., Nath, G., Unsteady Mixed Convection with Double Diffusion over a Horizontal Cylinder and a Sphere within a Porous Medium, *Wärme- Und Stoffübertragung,* 24(2), 1989, 103–109.
[24] Patil, P.M., Shashikant, A., Roy, S., Momoniat, E., Unsteady Mixed Convection over an Exponentially Decreasing External Flow Velocity, *International Journal of Heat and Mass Transfer,* 111(1), 2017, 643–650.
[25] Lewis, R.W., Morgan, K., Zienkiewicz, O.C., *Numerical Methods in Heat Transfer*, Wiley, New York, 1981.
[26] Patil, P.M., Shashikant, A., Roy, S., Hiremath, P.S., Mixed convection flow past a yawed cylinder, *International Communications in Heat and Mass Transfer*, 114(1), 2020, 104582.
[27] Meena, B. K., Nath, G., Nonsimilar Incompressible Laminar Boundary Layers with Magnetic Field, *Proceedings of the Indian Academy of Sciences - Section A,* 87(2), 1978, 55–64.
[28] Bin Ismail, M.A., Mohammad, N.F., Shafie, S., Unsteady Boundary Layer Flow of Sphere Filled with Nanofluid in the Present of Magnetic Fields, *Solid State Science and Technology VI*, 290(1), 2019, 314–322.
[29] Sathyakrishna, M., Roy, S., Nath, G., Unsteady Two-Dimensional and Axisymmetric MHD Boundary-Layer Flows, *Acta Mechanica,* 150(1), 2001, 67–77.
[30] Sheikholeslami, M., Shah, Z., Shafee, A., Khan, I., Tlili, I., Uniform magnetic force impact on water based nanofluid thermal behavior in a porous enclosure with ellipse shaped obstacle, *Scientific Reports*, 9(1), 2019, 1196.
[31] Aydin, O., Kaya, A., MHD Mixed Convection of a Viscous Dissipating Fluid about a Permeable Vertical Flat Plate, *Applied Mathematical Modelling,* 33(11), 2009, 4086–4096.
[32] Vajravelu, K., Li, R., Dewasurendra, M., Prasad, K.V., Mixed Convective Boundary Layer MHD Flow Along a Vertical Elastic Sheet, *International Journal of Applied and Computational Mathematics*, 3(3) 2017, 2501–2518.
[33] Roy, N., Gorla, R., Unsteady MHD Mixed Convection Flow of a Micropolar Fluid over a Vertical Wedge, *International Journal of Applied Mechanics and Engineering*, 22(2), 2017, 363–391.
[34] Patil, P.M., Shashikant, A., Momoniat, E., Unsteady MHD Mixed Convection along an Exponentially Stretching Surface: Impact of Opposing Buoyancy, *International Journal of Numerical Methods for Heat & Fluid Flow*, 28(12), 2018, 2769–2783.
[35] Seth, G.S., Sarkar, S., Unsteady Hydromagnetic Free Convection Flow Past an Impulsively Moving Vertical Plate with Newtonian Heating, *Journal of Nature Science and Sustainable Technology*, 8(1), 2014, 83–97.
[36] Safitri, O., Widodo, B., Adzkiya, D., Kamiran, K., Unsteady magnetohydrodynamics mixed convection flow pass sliced magnetic sphere in nano fluid, *AIP Conference Proceedings*, 2242(1), 2020, 030021.
[37] Anwar, T., Kumam, P., Watthayu, W., An exact analysis of unsteady MHD free convection flow of some nanofluids with ramped wall velocity and ramped wall temperature accounting heat radiation and injection/consumption, *Scientific Reports*, 10(1), 2020, 17830.
[38] Mahdy, A., Chamkha, A.J., Nabwey, H.A., Entropy analysis and unsteady MHD mixed convection stagnation-point flow of Casson nanofluid around a rotating sphere, *Alexandria Engineering Journal*, 59(3), 2020, 1693–1703.
[39] Alwawi, F.A., Alkasasbeh, H.T., Rashad, A.M., Idris, R., A Numerical Approach for the Heat Transfer Flow of Carboxymethyl Cellulose-Water Based Casson Nanofluid from a Solid Sphere Generated by Mixed Convection under the Influence of Lorentz Force, *Mathematics*, 8(7), 2020, 1094.
[40] Inouye, K., Tate, A., Finite-Difference Version of Quasi-Linearization Applied to Boundary-Layer Equations, *AIAA Journal,* 12(4), 1974, 558–560.
[41] Varga, S., *Matrix Iterative Analysis*, Springer-Verlag Berlin Heidelberg, 2000.

ORCID iD

A. Sahaya Jenifer https://orcid.org/0000-0002-7429-1416
P. Saikrishnan https://orcid.org/0000-0003-3087-3366

How to cite this article: Sahaya Jenifer A., Saikrishnan P., Lewis R.W. Unsteady MHD Mixed Convection Flow of Water over a Sphere with Mass Transfer, *J. Appl. Comput. Mech.*, 7(2), 2021, 935–943. https://doi.org/10.22055/JACM.2021.35920.2761